https://doi.org/10.5194/egusphere-2024-2271
Preprint. Discussion started: 29 July 2024

Observed bottom warming in the East Siberian Sea driven by the intensified vertical mixing

Xiaoyu Wang[1, 2, 3], Longjiang Mu[3], and Xianyao Chen[1, 2, 3, *]

[1] Frontier Science Center for Deep Ocean Multispheres and Earth System, Ocean University of China, Qingdao, China
[2] Physical Oceanography Laboratory, Ocean University of China, Qingdao, China
[3] Laoshan Laboratory, Qingdao, China

Correspondence to: Xianyao Chen (chenxy@ouc.edu.cn)

Abstract. The East Siberian Sea has the broadest continental shelf on Earth and nearly 80% of the subsea permafrost worldwide. There exists a cold layer with the temperature at freezing points around -1.5ºC above the sea floor of the shelf, preventing the heat transport from above to melt the permafrost and release the methane from sediments. However, we observed a worrying warming trend at the seafloor caused by enhanced vertical mixing in the shelf of the East Siberian Sea. In an ice-reduced Arctic continental shelf, even a moderate cyclone can result in the rapid growth of high wave to stir the marginal sea uniformly, which is not observed before. The intensified mixing can transport enormous heat downward, leading to a remarkable warming of more than 3°C at the bottom. As the Arctic is experiencing accelerated warming and the sea ice is rapidly retreating, the East Siberian Sea will undoubtedly suffer more extreme heatwaves, which might cause unpredictable climate impacts on the Arctic biochemical processes and greenhouse gas emission.

1 Introduction

The East Siberian Arctic shelf includes the Laptev Sea, the East Siberian Sea, and the Russian side of the Chukchi Sea. It is the broadest (~2.1×10^6 km^2) and shallowest (mean depth < 50 m) shelf in the world ocean, with nearly 80% of existing subsea permafrost and up to 50% CH_4 flux of the global coastal seas area (Shakhova et al., 2019; Sayedi et al., 2020). In summer, the seafloor of the East Siberian Arctic shelf is generally covered by cold bottom waters with several to tens of meters thick and temperatures close to the freezing point (Dmitrenko et al., 2010; Bauch & Cherniavskaia, 2018; Wang et al., 2021). This cold layer acts as a barrier to reduce the methane emissions from sediments by about half (Ferré et al., 2020; Altuna et al., 2021).

However, recent observations show that the near-bottom water over the Laptev Sea mid-shelf has exhibited pronounced warming due to the increasing downward heat transport during the retreat of the surface sea ice since mid-1980s (Janout & Lenn, 2014; Janout et al., 2016). In the later summer of 2007, the wind-induced vertical mixing caused a dramatic and abrupt near-bottom warming of about 3.0°C on the Laptev Sea mid-shelf (30-m water depth). The warming impacts on bottom water temperature anomaly remained for up to 3 months, leading to the warm bottom waters during the winter (Kraineva et al., 2019). A series of year-round oceanographic moorings at a deeper location (40-m water depth) in the Laptev

https://doi.org/10.5194/egusphere-2024-2271
Preprint. Discussion started: 29 July 2024

Sea recorded near-bottom temperatures reaching 2.0ºC during 2012/2013. Turbulent mixing is critical in determining vertical heat transfer in the water column. The strength of vertical mixing on the East Siberian Arctic shelf is dominated by wind forcing, tide-/shear-induced mixing, surface stress from ice motion, and buoyancy loss during ice formation. When the sea ice declines dramatically at the end of the summer melt season, wind forcing and tides become dominant roles. Previous studies showed that cyclone-induced strong wind can cause a mixing layer deepening of about 5 - 10 m (Long & Perrie, 2012; Peng et al., 2021). This slight deepening is intense enough to cause significant impacts on the thermal condition of the bottom layer on the inner shelf (water depth< 30 m).

The East Siberian Sea (ESS) has a much broader shelf than the Laptev Sea. However, due to the lack of in-situ observations, few observations and studies focus on bottom warming and related physical processes in the ESS. In the summer of 2016, the sea ice within the ESS sector decreased significantly, leaving a nearly ice-free shelf by early September (Figure 1). During this period, fieldwork in the ESS found that the whole water column on the mid-shelf was uniformly mixed and the bottom water temperature reaching nearly 3.0ºC. It is the first observations of such remarkable vertical mixing event in the ESS during the period with the most intensified upper stratification over the course of a year. This paper reports this extreme mixing event and the related processes. We also present the long-term vertical mixing intensification during the sea ice retreat and its thermal impacts on the bottom layer in the ESS in the recent decade.

2 Data and Methods

2.1 In-situ observations

The cruise (LA77), using the vessel R/V Akademik M.A. Lavrentyev, carried out two hydrographic sections across the ESS. The cross-shelf observations started at station LA77-17 on September 2, and ended at station LA77-40 on September 15. Twenty-three temperature-salinity profiles were obtained using an SBE-911 plus Conductivity, Temperature, and Depth (CTD) sensor with temperature and salinity accuracies of 0.001°C and 0.003, respectively. Nine temperature-salinity profiles were obtained using expendable CTD (XCTD) with temperature and salinity accuracies of 0.02°C and 0.04. The wind speed at each station was recorded by a mechanical anemometer mounted at about 10 m high.

2.2 Reanalysis product and satellite-derived data

We use the hourly and monthly atmospheric reanalysis products provided by the European Center for Medium-Range Weather Forecasts (ECMWF) (Hersbach et al., 2020). The spatial resolution of meteorological and heat flux datasets is 0.25° × 0.25°, and that of the ocean wave datasets is 0.5° × 0.5°.

We use the datasets of a Global Ocean Physics Reanalysis product (GLORYS12V1), with a spatial resolution of 1/12° × 1/12°, to investigate the variations of bottom water temperature and mixed layer depth. The GLORYS12V1, provided by the Copernicus Marine Environment Monitoring Service, is a data-assimilated eddy-resolving global

https://doi.org/10.5194/egusphere-2024-2271
Preprint. Discussion started: 29 July 2024

reanalysis based mainly on a real-time global forecasting system. In-situ observations, remotely sensed SST, sea ice concentration, and along-track altimeter data are jointly assimilated. The Copernicus Marine Environment Monitoring Service also provides surface velocities derived from absolute dynamic topography.

The sea surface temperature is from the Optimally Interpolated SST daily product v5.1 with a spatial resolution of 0.25° × 0.25°, supported by Remote Sensing Systems sponsored by National Oceanographic Partnership Program (NOPP) and the NASA Earth Science Physical Oceanography Program.

2.3 Mixed layer depth, wavelength, and ocean heat content

The method defining mixed layer depth (MLD) is according to the maximum depth at which the density is within a certain threshold of the shallowest measured density. Due to complex hydrographic conditions around the Arctic Ocean, there are various thresholds from 0.01 to 0.25 kg/m^3 (Timmermans et al., 2012; Peralta-Ferriz and Woodgate, 2015). In this study, we use a threshold value of 0.05 kg/m^3 to detect the rich vertical structures caused by water advection and the vertical mixing. Note that the other threshold density values would not make a difference in determining the extreme mixing event.

The wavelength λ is calculated using equations derived from the dispersion relation of regular waves (Holthuijsen, 2007), as follows:

$$\lambda=\frac{gT^2}{2\pi} \quad \text{when } d/\lambda \geq 0.5,$$

$$\lambda=\frac{gT^2}{2\pi}\tanh\left(\frac{2\pi d}{\lambda}\right) \quad \text{when } 0.05 \leq d/\lambda < 0.5,$$

$$\lambda=\sqrt{gd}\times T \quad \text{when } d/\lambda \leq 0.05,$$

where d is the water depth in meters, T the wave period in seconds, and g the acceleration of gravity, 9.8 m/s^2.

Ocean heat content Q is calculated for the surface and bottom layers as follows:

$$Q=\int_{z_1}^{z_2}\rho C_p(\theta-\theta_{fz})d_z,$$

where ρ is average water density (~1026 kg/m^3), C_p seawater heat capacity (~4200 J/(kg·°C), θ and θ_{fz} the potential temperature and freezing point (°C) of each layer, respectively, and z_1 and z_2 the depth range of each layer.

2.4 Days with heavy winds and high waves

Energy induced by heavy winds and high ocean waves are primary factors that enhance the diapycnal mixing in the upper ocean. We determine the days with heavy winds and high wave following three criteria: First, the local (in one grid) hourly wind speed is higher than 13 m/s, and its cumulative duration within one day is more than 6 hours; Second, the grids with the wind speed higher than the criteria will occupy at least 20% of the total area of the studied region (155–174.5ºE, 71.5–74.5°N); Third, for the days with high waves, its hourly significant wave height must be higher than 2.4 m.

https://doi.org/10.5194/egusphere-2024-2271
Preprint. Discussion started: 29 July 2024

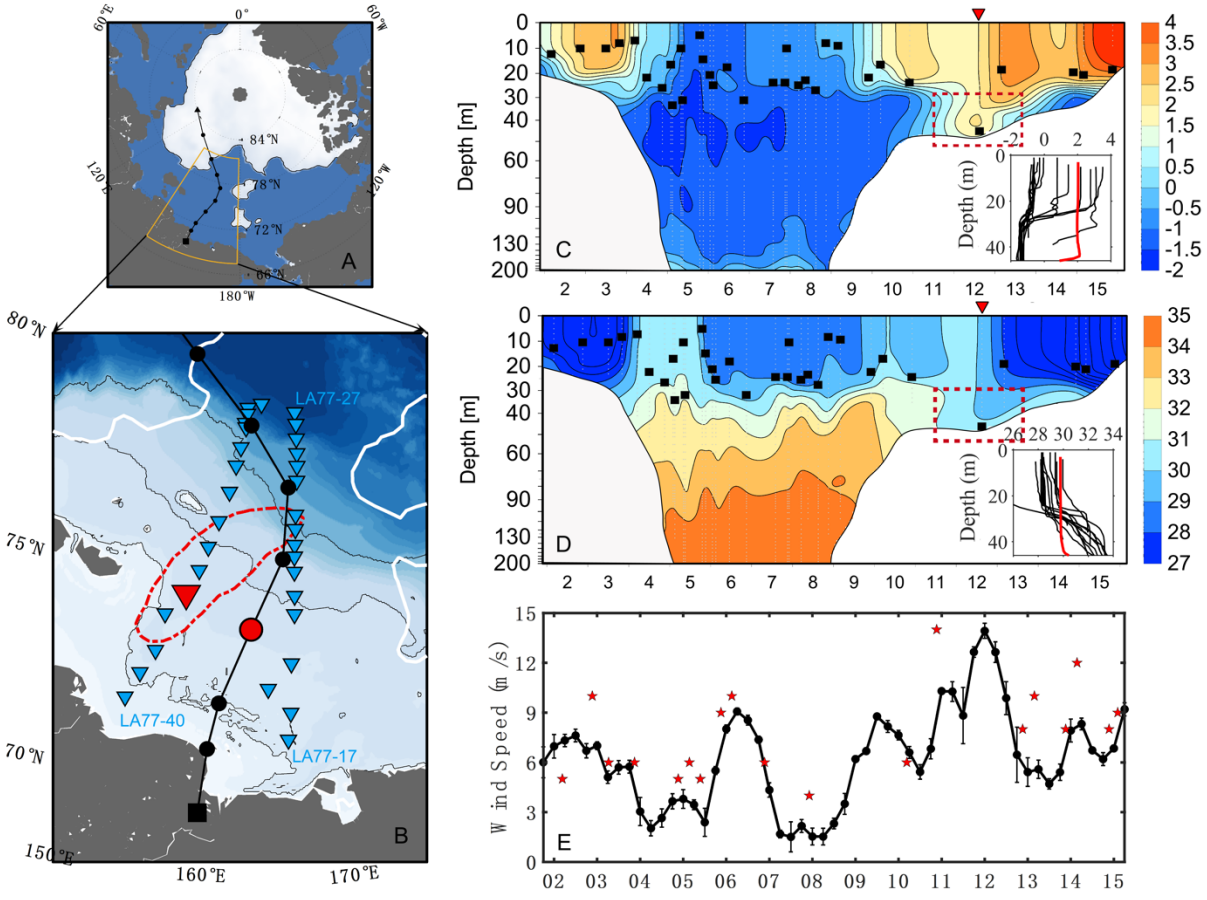

Figure 1: Observations in the East Siberian Sea (ESS).

(**a**) The path of the Arctic cyclone from 9 to 12, 2016. The white area indicates the ocean covered by sea ice. (**b**) Observation station locations (blue triangles) in the ESS. The red triangle marks the station LA77-35. Dots show the trajectory of the cyclone center. The red dashed line marks the area with wind speed exceeding 12 m/s. (**c**) The temperature along the section from LA77-17 to LA77-27 and then from LA77-28 to LA77-40. The horizontal coordinate is time. The black square rectangles denote the mixed layer depth at each station, and the red triangle marks the location of station LA77-35. The blue rectangular box marks where the significant bottom water warming occurs. (**d**) Same as (**c**) but for the salinity. (**e**) Variation of wind speeds during the observation period. Black dots denote the 6-hour wind speeds derived from the hourly ERA5 reanalysis data according to the vessel's GPS positions. The red asterisks denote in-situ observations of wind speeds from an onboard anemometer.

https://doi.org/10.5194/egusphere-2024-2271
Preprint. Discussion started: 29 July 2024

3 Results

3.1 A record deepening of the surface mixed layer in Summer

Observations in September 2016 showed that the water column on the ESS shelf has a two-layer structure: the surface mixed layer and the bottom layer separated by the seasonal pycnocline. Temperatures in the surface mixed layer were between 2–5°C, and the salinity was lower than 31.0, while the temperatures in the bottom layer dropped below -1°C, and the salinity ranged between 31.0–34.0. The mixed layer depth was only 10–20 m on the mid-shelf, and about 30 m near the slope. However, observation at LA77-35 showed that the mixed layer deepened to the sea floor, resulting in a uniform water column of 45 m thick. At the same time, the bottom water temperature increased to about 2°C, above the freezing point. Because station LA77-35 was far from the influences of Atlantic Water and coastal river plumes, we deduce that the unusual bottom warming at LA77-35 was due to intense diapycnal mixing from the surface layer.

From September 9 to 12, 2016, a synoptic-scale Arctic cyclone moved southward across the ESS shelf (Figure 1a) with open water about 1100 km long along its path. When its center moved to the mid-shelf on September 11, the cyclone caused strong winds in the western ESS. Station LA77-35 was right in the center of heaviest wind, where the observed wind speed exceeded 14 m/s on September 11. The CTD profile of LA77-35 was obtained on September 12 when the sea condition calmed down. Hence the observed ocean state at LA77-35 represented the final influences of the cyclone on the mid-shelf. The extreme deepening of the mixed layer at LA77-35 was driven by the windy weather condition. The intense diapycnal mixing completely eroded the stratification on the shelf, resulting in a record deepening of the mixed layer in the Pacific sector of the Arctic Ocean during summertime.

3.2 Vertical mixing intensified by the growing waves in open water

The sea level pressure at the center of the cyclone was 1012–1024 hPa, indicating it was just a moderate cyclone, compared with the minimum observed sea level pressures during two Arctic cyclones in August 2016 (967 hPa) and August 2008 (976 hPa), respectively (Long & Perrie, 2012; Peng et al., 2021). The resulting maximum wind speed was also lower than the previous two. However, the deepened mixed layer observed in September 2016 in the ESS reached about 25 m depth, much larger than the 5–10 m deepening reported by previous studies. The main difference between the cyclone we experienced during September 9-12, 2016, and the reported ones was that its path was along the entirely open waters, allowing the growing of the wave and the continuous wind energy input into the ocean.

At 00:00 UTC on September 11, when the cyclone center was still in the Arctic basin, the significant wave height (using wave height for short in the following text) near the continental slope was about 1.5 m (Figure 2a). Half a day later when the cyclone center moved southward onto the outer shelf, the maximum wave height gradually grew to about 2.0 m. When the cyclone landed on September 12, nearly all the wave heights on the western ESS shelf were above 2.0 m. The maximum wave height exceeded 3.0 m, and its location was close to station LA77-35 (Figure 2c).

https://doi.org/10.5194/egusphere-2024-2271
Preprint. Discussion started: 29 July 2024

The turbulent mixing induced by wave breaking is mainly confined within the near-surface zone with the depth scale of wave heights (Soloviev & Lukas, 2003; Sulisz et al., 2015). To examine whether the wave-induced mixing can reach the seafloor of the mid-shelf, we calculated the wavelength change during the cyclone's passing (Figure 2d–f). On September 12, the wavelength in the mid-shelf region with 30 to 60 m depths increased to about 70 m, long enough to stir the whole water column by enhanced shearing and wave breaking. The well-developed waves enhanced turbulent mixing in the mid-shelf, significantly deepening the mixed layer, and fully eroding the summer ocean stratification from surface to bottom. Therefore, although the cyclone we experienced was limited in intensity, its wind energy input to the ocean is maximal accumulation along the large areas of open waters from north to south.

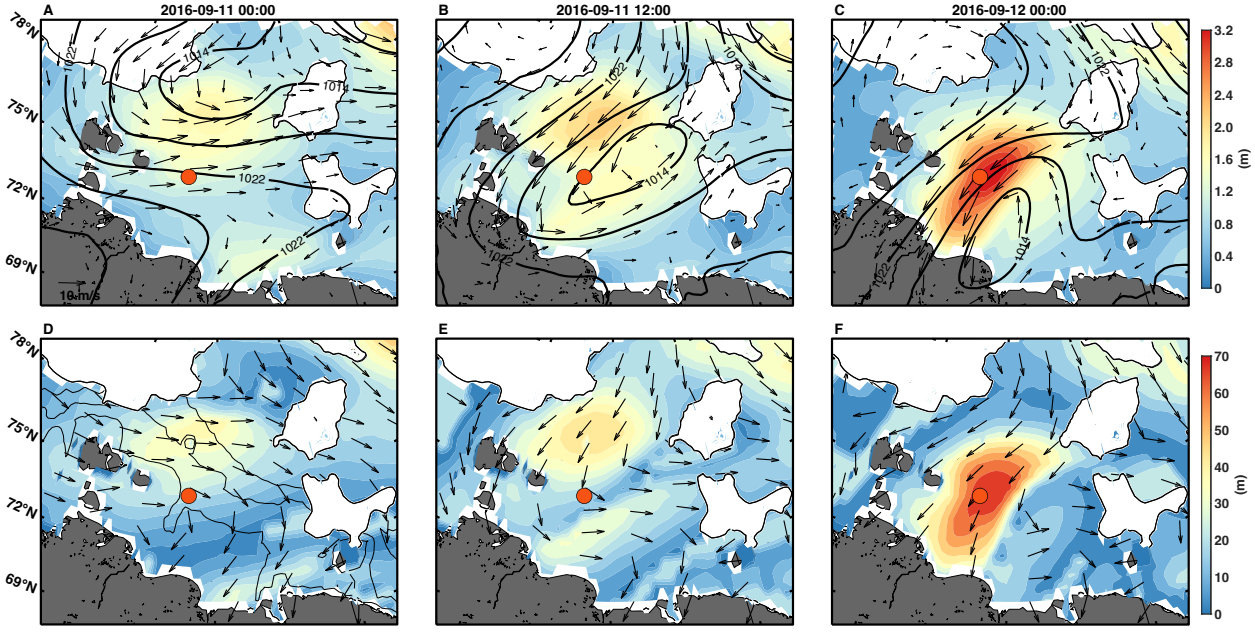

Figure 2: Distribution of significant wave height every 12 hours.

(**a-c**) From September 11 to 12. The black contours represent sea level pressure in units of hPa. The arrows represent the 10 m wind field. The white area denotes sea ice extent, and the red asterisk marks the location of station LA-77-35. (**d-f**) Same as top but for the distribution of wavelength. Arrows indicate the wave direction. Thin black lines in (**d-f**) indicate 30 m, 50 m, and 100 m isobath, respectively.

https://doi.org/10.5194/egusphere-2024-2271
Preprint. Discussion started: 29 July 2024

3.3 Heat Transfer to the bottom of mid-shelf by intensified vertical mixing

Observations showed that the mixed layer depth in the ESS in early September was only 15 - 25 m, and water temperatures in the bottom layer were below -1°C (Figure 1c). However, the wind-induced diapycnal mixing at station LA77-35 caused a remarking warming of about 3°C near the seafloor of the mid-shelf. This intensified downward mixing process transferred about 1.9×108 J/m^2 of heat from the surface to the bottom layer, equivalent to a monthly mean heat flux around 73 W/m^2, an order of magnitude higher than the net solar radiation reaching the bottom during summertime.

During September 10-11, the SST at station LA77-35 decreased by about 1.2°C (Figure 3a). This rapid decrease in temperature was associated with the enhanced diapycnal mixing caused by the cyclone, as well as the enhanced surface heat flux from the ocean to the atmosphere. According to the ERA5 Reanalysis data, the net shortwave radiation decreased to about 40 W/m^2 in this region (positive value means heat input to the ocean), the sensible and latent heat fluxes at station LA77-35 increased to -40 W/m^2 and -50 W/m^2, respectively (Figure 3b). The net surface heat flux surface was about -73 W/m^2, which can result in the SST decrease of about 0.15-0.19°C within two days, if assuming a mixed layer depth of 15-20 m before the cyclone. The SST at station LA77-35 decreased by more than 1.0°C, and the area around the station with the same cooling rate was about 14,000 km^2, suggesting the area with the significant surface cooling most likely experienced the same-extent bottom warming induced by intensified vertical mixing, as observed at LA77-35.

It should be noted that the net surface heat flux, about 45 W/m^2 during September 10 to 12 can lead to more than 2°C reduction of the SST, if assuming the mixed layer thickness is about 20 m, whereas the SST at station LA77-35 only decreased by about 1.2°C. We infer that the additional heat is from the advection of the warming coastal water in the west of the ESS to the mid-shelf. But the heat advection only explains about 30-40% of the surface and the mixed layer temperature variability, the vertical heat transport enhanced by the vertical mixing still dominants the bottom warming in this area.

https://doi.org/10.5194/egusphere-2024-2271
Preprint. Discussion started: 29 July 2024

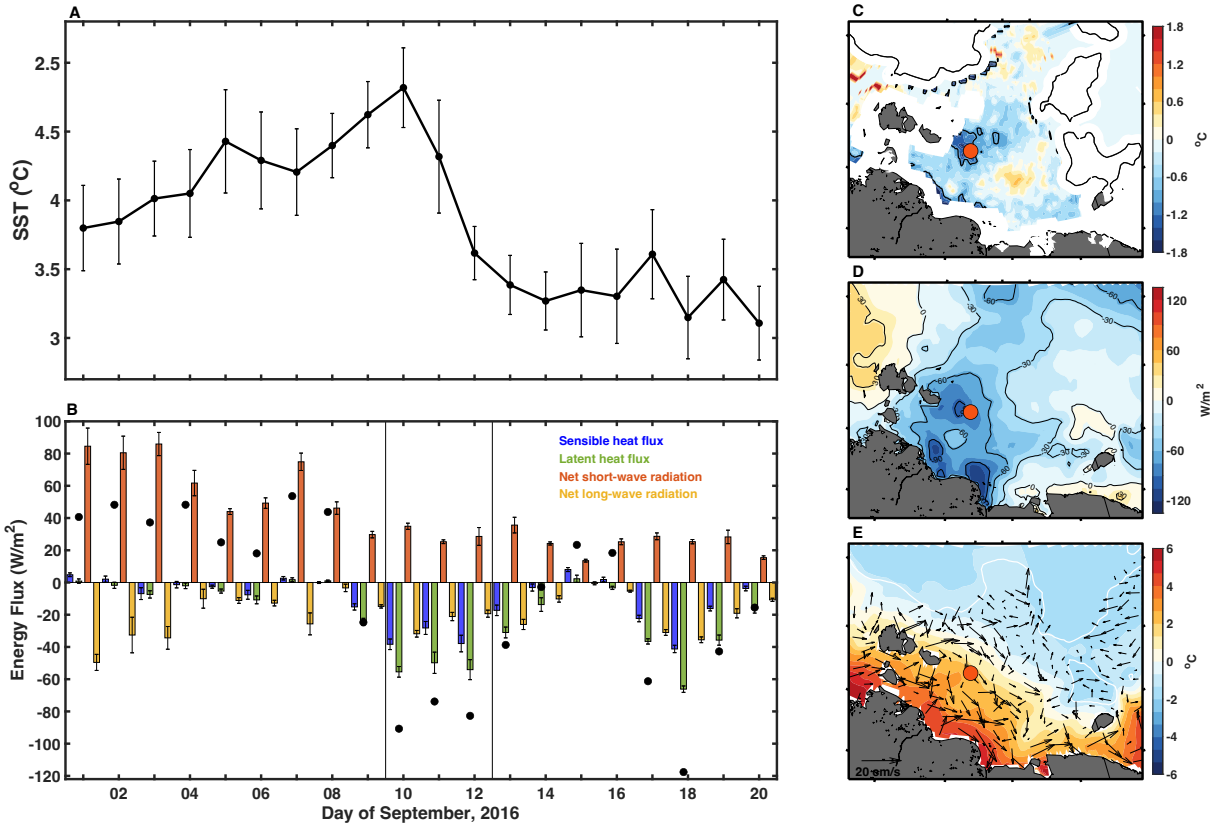

Figure 3: Sea surface temperature (SST), air-sea energy flux, and the surface geostrophic current in the ESS.

(**a**) Changes of mean SST in the region around station LA77-35 (74.375–74.875°N，157.125–157.875°E); (**b**) Same as (**a**) but for the mean air-sea energy fluxes. Positive value means heat input into the ocean. Black dots denote the net surface energy flux. (**c**) Difference of the SST between September 10 and 12. The red asterisk marks the location of station LA77-35. (**d**) Distribution of mean surface energy balance between September 10 to 12. (**e**) Same as (**d**) but for the mean surface geostrophic current (derived from sea surface height) and SST during the observation period.

3.4 Intensification of the wind-induced mixing on the ESS shelf

We further investigate the long-term trend of wind-induced mixing in the ESS during the recent decade. The key parameters include the sea ice extent, the day with heavy winds and high waves, the mixed layer depth, and the bottom water temperature (Figure 4). The sea ice extent became lower than 0.5×10^6 km^2 since 2007, and remained at similar level since then (Figure 4a). Simultaneously, the number of days with heavy winds and high waves gradually increased. All of the top

https://doi.org/10.5194/egusphere-2024-2271
Preprint. Discussion started: 29 July 2024

five years with the most prevailing windy processes occur in recent decade. Especially, in September 2016 and 2017, heavy winds and high waves prevailed in the ESS for more than a week (Figure 4b). As a result, the mean mixed layer depth in September exhibits significant deepening trend from about 11 m to nearly 15 m during last two decades (Figure 4c), and the bottom temperature reaches nearly 0℃ during 2015 and 2016, indicating an increasing influence of wind-induced synoptic processes on vertical mixing (Figure 4d).

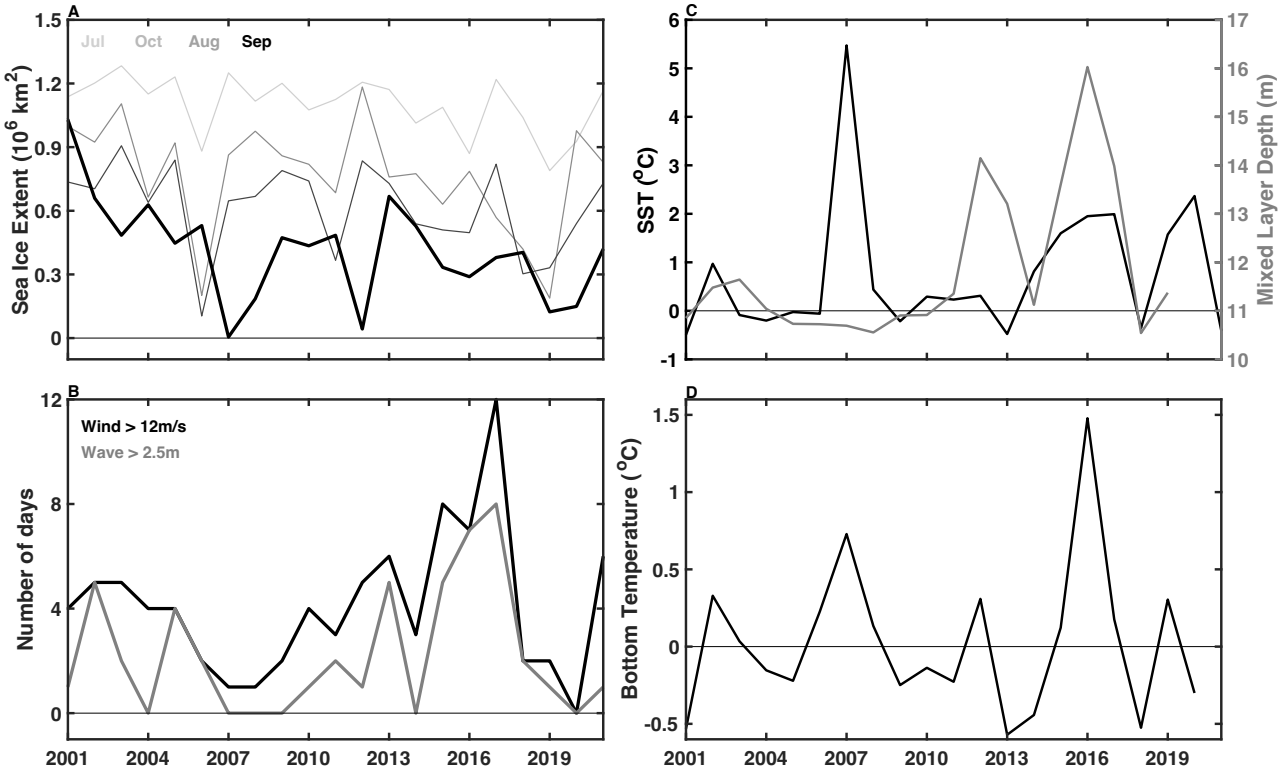

Figure 4: Variability of the sea ice extent, number of days with heavy winds and high waves, SST, and the bottom water temperature in the ESS during 2001-2021.

(**a**) Variation of sea ice extent in July, August, September (thick black line), and October in 2016. (**b**) Number of days with heavy winds and high waves. (**c**) SST and the mixed layer depth in the ESS in summer. (**d**) Same as (**c**) but for the bottom water temperature.

https://doi.org/10.5194/egusphere-2024-2271
Preprint. Discussion started: 29 July 2024

4 Discussion and conclusions

Deep water mixing can rapidly ventilate bubble-transported and dissolved methane from the bottom layer, producing high emission rates to the atmosphere (Shakhova et al., 2014; James et al., 2016). Previous studies reported that summer cyclones can deepen the surface mixed layer of the Arctic Ocean by 5 - 10 m, still away from the seafloor (Long & Perrie, 2012; Peng et al., 2021). Here we show an event with a thickened mixed layer to the seafloor with a 25 m depth in the ESS. This recorded-deepening of the mixed layer in the Pacific sector results from an Arctic cyclone moving onto the shelf from open waters with nearly a thousand kilometers from north to south. Over such large open water area, the wave can grow sufficiently and become strong enough to strengthen the vertical mixing of the mid-shelf ocean. The intensified mixing transports a large amount of heat from the upper layer straightly to the seafloor, leading to remarkable warming of about 3°C in the bottom layer. Our observational study provides an important supplement and extension of previous knowledge of wind-induced bottom water warming in the Laptev Sea shelf (Hölemann et al., 2011; Janout et al., 2016; Kraineva et al., 2019). Furthermore, based on the in-situ observations, we estimate that the area of bottom water warming on the mid-shelf can at least reach about 14,000 km^2.

The Arctic has warmed nearly 2-4 times faster than the global average since 1979 (Serreze & Barry, 2011; Rantanen et al., 2022). At the same time, the summer sea ice covering the Arctic shelves also decreased dramatically and remained at a low level since 2007 (Park et al., 2020; Liu et al., 2021). Lengthening summers, reduced sea ice extent, and increasing solar heating are pushing more heat into the ocean (Angelopoulos et al., 2020; Dong et al., 2022). With the increasing trends of the open-water area, heavy wind days, and high wave days during summertime since 2012, more vigorous wind-induced mixing and the enhanced bottom warming will happen in the ESS. Now the average bottom water temperature in summer is still below 0°C. However, with the further reduction of sea ice extent and increasing heat content in the mixed layer in the future, the bottom water temperature will undoubtedly become warmer than the freezing point, which is very serious for the bottom permafrost and the methane buried in the sediments. Previous studies report that temperatures of the surface sediments in the ESS remain at about -1.5 to -1.8°C (Chuvilin et al., 2021; 2022), slightly colder than bottom water temperatures in summer. It indicates that the heat entering the bottom layer by wind-induced mixing will continue to enter the sediments, eventually causing the sediment temperature to deviate from the freezing point, which will accelerate subsea methane emissions (Sultan et al., 2020; Wild et al., 2022;). Quantifying the impact of these processes is beyond the scope of this paper, but it deserves attention in the future.

Observations in the Laptev Sea revealed that the near-bottom warming could remain for at least 2–3 months when the sea ice refreezes again (Kraineva et al., 2019). This means that the heat stored in the bottom layer during summertime can partly return to the surface layer to melt ice. Unfortunately, the lack of long-term mooring observations prevents us from evaluating how many proportions of heat can reemerge to melt sea ice in the following winter in the ESS. Analyzing and quantifying the vertical distribution and transport of ocean heat on the Arctic shelves will improve the understanding of the

https://doi.org/10.5194/egusphere-2024-2271
Preprint. Discussion started: 29 July 2024

impacts of the Arctic Ocean warming on regional climate changes. To address this question, long-term mooring systems are urgently needed to monitor the ocean-seabed thermal processes in the ESS.

Competing interests

The contact author has declared that none of the authors has any competing interests.

Acknowledgments

This study is supported by the National Key R&D Program of China under Grant 2019YFA0607000，the Chinese Natural Science Foundation under Grants 42276248 and 42176235. The authors would like to thank the European Center for Medium-Range Weather Forecasts for access to the ERA5 reanalysis data, the National Oceanographic Partnership Program (NOPP) and the NASA Earth Science Physical Oceanography Program for access to the Optimally Interpolated SST data, the Copernicus Marine Environment Monitoring Service (CMEMS) for access to the Global Ocean Physics Reanalysis product and the surface geostrophic current data.

The in-situ observation data and the detail introductions are available at https://doi.org/10.5281/zenodo.4507584.

The ERA5 hourly and monthly data are available at https://doi.org/10.24381/cds.adbb2d47 and https://doi.org/10.24381/cds.f17050d7.

The Microwave Optimally Interpolated SST data are produced by Remote Sensing Systems and are available at https://www.remss.com/measurements/sea-surface-temperature/.

The Global Ocean Physics Reanalysis product is available at https://doi.org/10.48670/moi-00021, and the surface geostrophic current data are available at https://doi.org/10.48670/moi-00148.

References

Angelopoulos, M., Overduin, P. P., Miesner, F., Grigoriev, M. N., & Vasiliev, A. A. Recent advances in the study of Arctic submarine permafrost. *Permafrost and Periglacial Processes*, *31*(3), 442-453. https://doi.org/10.1002/ppp.2061, 2020.

Bauch, D., & Cherniavskaia, E. Water Mass Classification on a Highly Variable Arctic Shelf Region: Origin of Laptev Sea Water Masses and Implications for the Nutrient Budget. *Journal of Geophysical Research: Oceans*, *123*(3), 1896-1906. https://doi.org/10.1002/2017JC013524, 2018.

Chuvilin, E., Bukhanov, B., Grebenkin, S., Tumskoy, V., Shakhova, N., Dudarev, O., Semiletov, I., & Spasennykh, M. Thermal properties of sediments in the East Siberian Arctic Seas: A case study in the Buor-Khaya Bay. *Marine and Petroleum Geology*, *123*, 104672. https://doi.org/10.1016/ j.marpetgeo.2020.104672, 2021.

https://doi.org/10.5194/egusphere-2024-2271
Preprint. Discussion started: 29 July 2024

Chuvilin, E., Bukhanov, B., Yurchenko, A., Davletshina, D., Shakhova, N., Spivak, E., Rusakov, V., Dudarev, O., Khaustova, N., Tikhonova, A., Gustafsson, O., Tesi, T., Martens, J., Jakobsson, M., Spasennykh, M., & Semiletov, I. In-situ temperatures and thermal properties of the East Siberian Arctic shelf sediments: Key input for understanding the dynamics of subsea permafrost. *Marine and Petroleum Geology*, *138*, 105550. https://doi.org/10.1016/j.marpetgeo.2022.105550, 2022.

Dmitrenko, I. A., Kirillov, S. A., Tremblay, L. B., Kassens, H., Anisimov, O. A., Lavrov, S. A., Razumov, S. O., & Grigoriev, M. N. Recent changes in shelf hydrography in the Siberian Arctic: Potential for subsea permafrost instability. *Journal of Geophysical Research: Oceans*, *116*(C10) https://doi.org/10.1029/2011JC007218, 2011.

Dong, J., Shi, X., Gong, X., Astakhov, A. S., Hu, L., Liu, X., Yang, G., Wang, Y., Vasilenko, Y., Qiao, S., Bosin, A., & Lohmann, G. Enhanced Arctic sea ice melting controlled by larger heat discharge of mid-Holocene rivers. *Nature Communications*, *13*(1), 5368. http://doi.org/10.1038/s41467-022-33106-1, 2022.

El Bani Altuna, N., Rasmussen, T. L., Ezat, M. M., Vadakkepuliyambatta, S., Groeneveld, J., & Greaves, M. Deglacial bottom water warming intensified Arctic methane seepage in the NW Barents Sea. *Communications Earth & Environment*, *2*(1), 188. http://doi.org/10.1038/s43247-021-00264-x, 2021.

Ferré, B., Jansson, P. G., Moser, M., Serov, P., Portnov, A., Graves, C. A., Panieri, G., Gründger, F., Berndt, C., Lehmann, M. F., & Niemann, H. Reduced methane seepage from Arctic sediments during cold bottom-water conditions. *Nature Geoscience*, *13*(2), 144-148. http://doi.org/10.1038/s41561-019-0515-3, 2020.

Hersbach, H., Bell, B., Berrisford, P., Hirahara, S., Horányi, A., Muñoz-Sabater, J., Nicolas, J., Peubey, C., Radu, R., Schepers, D., Simmons, A., Soci, C., Abdalla, S., Abellan, X., Balsamo, G., Bechtold, P., Biavati, G., Bidlot, J., Bonavita, M., De Chiara, G., Dahlgren, P., Dee, D., Diamantakis, M., Dragani, R., Flemming, J., Forbes, R., Fuentes, M., Geer, A., Haimberger, L., Healy, S., Hogan, R. J., Hólm, E., Janisková, M., Keeley, S., Laloyaux, P., Lopez, P., Lupu, C., Radnoti, G., de Rosnay, P., Rozum, I., Vamborg, F., Villaume, S., & Thépaut, J. The ERA5 global reanalysis. *Quarterly Journal of the Royal Meteorological Society*, *146*(730), 1999-2049. https://doi.org/10.1002/qj.3803, 2020.

Hölemann, J. A., Kirillov, S., Klagge, T., Novikhin, A., Kassens, H., & Timokhov, L. Near-bottom water warming in the Laptev Sea in response to atmospheric and sea-ice conditions in 2007. *Polar Research*, http://doi.org/10.3402/polar.v30i0.6425, 2011.

Holthuijsen, L. H. *Waves in oceanic and coastal waters*, Cambridge university press, https://doi.org/10.1017/CBO9780511618536, 2007.

James, R. H., Bousquet, P., Bussmann, I., Haeckel, M., Kipfer, R., Leifer, I., Niemann, H., Ostrovsky, I., Piskozub, J., Rehder, G., Treude, T., Vielstädte, L., & Greinert, J. Effects of climate change on methane emissions from seafloor sediments in the Arctic Ocean: A review. *Limnology and Oceanography*, *61*(S1), S283-S299. https://doi.org/10.1002/lno.10307, 2016.

Janout, M. A., & Lenn, Y. Semidiurnal Tides on the Laptev Sea Shelf with Implications for Shear and Vertical Mixing. *Journal of Physical Oceanography*, *44*(1), 202-219. http://doi.org/10.1175/JPO-D-12-0240.1, 2014.

https://doi.org/10.5194/egusphere-2024-2271
Preprint. Discussion started: 29 July 2024

Janout, M., Hölemann, J., Juhls, B., Krumpen, T., Rabe, B., Bauch, D., Wegner, C., Kassens, H., & Timokhov, L. Episodic warming of near-bottom waters under the Arctic sea ice on the central Laptev Sea shelf. *Geophysical Research Letter*, *43*(1), 264-272. https://doi.org/10.1002/2015GL066565, 2016.

Kraineva, M., Golubeva, E., & Platov, G.. Simulation of the near-bottom water warming in the Laptev Sea in 2007–2008. *Bull. Nov. Comp. Center Num. Model. in Atmosph*, 17, 21-30, 2019.

Liu, Z., Risi, C., Codron, F., He, X., Poulsen, C. J., Wei, Z., Chen, D., Li, S., & Bowen, G. J. Acceleration of western Arctic sea ice loss linked to the Pacific North American pattern. *Nature Communications*, *12*(1), 1519. http://doi.org/10.1038/s41467-021-21830-z, 2021.

Long, Z., & Perrie, W. Air-sea interactions during an Arctic storm. Journal of *Geophysical Research: Atmospheres*, *117*(D15) https://doi.org/10.1029/2011JD016985, 2012.

Park, H., Watanabe, E., Kim, Y., Polyakov, I., Oshima, K., Zhang, X., Kimball, J. S., & Yang, D. Increasing riverine heat influx triggers Arctic sea ice decline and oceanic and atmospheric warming. *Science Advances*, *6*(45), c4699. http://doi.org/doi:10.1126/sciadv.abc4699, 2020.

Peng, L., Zhang, X., Kim, J., Cho, K., Kim, B., Wang, Z., & Tang, H. Role of Intense Arctic Storm in Accelerating Summer Sea Ice Melt: An In Situ Observational Study. *Geophysical Research Letter*, *48*(8), e2021G-e92714G. https://doi.org/10.1029/2021GL092714, 2021.

Peralta-Ferriz, C., & Woodgate, R. A. Seasonal and interannual variability of pan-Arctic surface mixed layer properties from 1979 to 2012 from hydrographic data, and the dominance of stratification for multiyear mixed layer depth shoaling. *Progress in Oceanography*, *134*, 19-53. https://doi.org/10.1016/j.pocean.2014.12.005, 2015.

Rantanen, M., Karpechko, A. Y., Lipponen, A., Nordling, K., Hyvärinen, O., Ruosteenoja, K., Vihma, T., & Laaksonen, A. The Arctic has warmed nearly four times faster than the globe since 1979. *Communications Earth & Environment*, *3*(1), 168. http://doi.org/10.1038/s43247-022-00498-3, 2022.

Sayedi, S. S., Abbott, B. W., Thornton, B. F., Frederick, J. M., Vonk, J. E., Overduin, P., Schädel, C., Schuur, E. A. G., Bourbonnais, A., Demidov, N., Gavrilov, A., He, S., Hugelius, G., Jakobsson, M., Jones, M. C., Joung, D., Kraev, G., Macdonald, R. W., David McGuire, A., Mu, C., O Regan, M., Schreiner, K. M., Stranne, C., Pizhankova, E., Vasiliev, A., Westermann, S., Zarnetske, J. P., Zhang, T., Ghandehari, M., Baeumler, S., Brown, B. C., & Frei, R. J. Subsea permafrost carbon stocks and climate change sensitivity estimated by expert assessment. *Environmental Research Letters*, *15*(12), 124075. http://doi.org/10.1088/1748-9326/abcc29, 2020.

Serreze, M. C., & Barry, R. G. Processes and impacts of Arctic amplification: A research synthesis. *Global and Planetary Change*, *77*(1), 85-96. https://doi.org/10.1016/j.gloplacha.2011.03.004, 2011.

Shakhova, N., Semiletov, I., Leifer, I., Sergienko, V., Salyuk, A., Kosmach, D., Chernykh, D., Stubbs, C., Nicolsky, D., Tumskoy, V., & Gustafsson, Ö. Ebullition and storm-induced methane release from the East Siberian Arctic Shelf. *Nature Geoscience*, *7*(1), 64-70. http://doi.org/10.1038/ngeo2007, 2014.

https://doi.org/10.5194/egusphere-2024-2271
Preprint. Discussion started: 29 July 2024

Shakhova, N., Semiletov, I., & Chuvilin, E. Understanding the Permafrost–Hydrate System and Associated Methane Releases in the East Siberian Arctic Shelf. *Geosciences*, *9*(6), 251, 2019.

Soloviev, A., & Lukas, R. Observation of wave-enhanced turbulence in the near-surface layer of the ocean during TOGA COARE. *Deep Sea Research Part I: Oceanographic Research Papers*, *50*(3), 371-395. https://doi.org/10.1016/S0967-0637(03)00004-9, 2003.

Sulisz, W., Paprota, M., & Wang, J. Theoretical and Experimental Investigations of Wave-Induced Vertical Mixing. *Mathematical Problems in Engineering*, 950849. http://doi.org/10.1155/2015/950849, 2015.

Sultan, N., Plaza-Faverola, A., Vadakkepuliyambatta, S., Buenz, S., & Knies, J. Impact of tides and sea-level on deep-sea Arctic methane emissions. *Nature Communications*, *11*(1), 5087. http://doi.org/10.1038/s41467-020-18899-3, 2020.

Timmermans, M., Cole, S., & Toole, J. Horizontal Density Structure and Restratification of the Arctic Ocean Surface Layer. *Journal of Physical Oceanography*, *42*(4), 659-668. http://doi.org/10.1175/JPO-D-11-0125.1, 2012.

Wang, X., Zhao, J., Lobanov, V. B., Kaplunenko, D., Rudykh, Y. N., He, Y., & Chen, X. Distribution and Transport of Water Masses in the East Siberian Sea and Their Impacts on the Arctic Halocline. *Journal of Geophysical Research: Oceans*, *126*(8), e2020J-e16523J. https://doi.org/10.1029/2020JC016523, 2021.

Wild, B., Shakhova, N., Dudarev, O., Ruban, A., Kosmach, D., Tumskoy, V., Tesi, T., Grimm, H., Nybom, I., Matsubara, F., Alexanderson, H., Jakobsson, M., Mazurov, A., Semiletov, I., & Gustafsson, Ö. Organic matter composition and greenhouse gas production of thawing subsea permafrost in the Laptev Sea. *Nature Communications*, *13*(1), 5057. http://doi.org/10.1038/s41467-022-32696-0, 2022.